# Out-of-Plane Orbital Characters of Intrinsic and Doped Holes in $\mathrm{La_{2-x}Sr_xCuO_4}$

C. T. Chen, L. H. Tjeng, J. Kwo, H. L. Kao, P. Rudolf, F. Sette, and R. M. Fleming
*AT&T Bell Laboratories, 600 Mountain Avenue, Murray Hill, New Jersey 07974*
(Received 18 February 1992)

Bulk-sensitive, polarization-dependent O $K$- and Cu $L$-edge absorption spectra of single-domain $\mathrm{La_{2-x}Sr_xCuO_4}$ with $\mathrm{CuO_2}$ planes tilted off the sample surface were measured. A novel experimental configuration was utilized to achieve complete polarization geometry and eliminate optical path variations. Contrary to previous measurements, our data show for both intrinsic and doped holes a significant amount of O $2p_z$ character, likely associated with apical O, but a very weak Cu $3d_{3z^2-r^2}$ character. These results impose strong constraints on superconductivity models invoking out-of-plane orbitals, and suggest that the apical O $2p_z$ orbital may play an important role in high-$T_c$ phenomena.

PACS numbers: 78.70.Dm, 74.65.+n, 74.70.Vy

The electronic structure of high-$T_c$ superconducting cuprates has been intensively studied using electron spectroscopy techniques [1]. In particular, polarized inner-shell absorption measurements have provided valuable information on the local orbital character of the carriers in hole-doped cuprates [2-4]. These conducting holes were determined to contain predominately in-plane O $2p_{x,y}$ and Cu $3d_{x^2-y^2}$ orbital characters, thus supporting the two-dimensional nature of high-$T_c$ superconductivity. However, anomalies in the lattice dynamics have been interpreted to favor some out-of-plane orbitals [5], and a variety of models for the superconductivity have been proposed in which Cu $3d_{3z^2-r^2}$ and/or apical O $2p_z$ orbitals play a key role [6-8]. On the other hand, a negative influence of the out-of-plane orbitals on superconductivity has been suggested recently [9]. So far, most of the polarized x-ray absorption and electron energy loss measurements have reported on the Cu $3d_{3z^2-r^2}$ character of the conducting holes. Because of differences in surface chemistry and spectroscopic probing depth, these experiments, using samples with the $\mathrm{CuO_2}$ planes parallel to the surface, suffered from inevitable changes in surface sensitivity when measuring polarization dependency. Marked inconsistency has been found with a Cu $3d_{3z^2-r^2}$ to $3d_{x^2-y^2}$ intensity ratio ranging from 5% to 20%, either with or without an energy shift [2,3]. Several polarized O $K$-edge absorption measurements have been reported but show no conclusive evidence for the presence of the apical O $2p_z$ character except for the special case of $\mathrm{YBa_2Cu_3O_7}$ where holes in the chains were measured [3,4].

In order to identify out-of-plane orbitals, and to help elucidate its relevancy to high-$T_c$ superconductivity, we have performed high-precision, bulk-sensitive, polarization-dependent fluorescence yield absorption measurements on $\mathrm{La_{2-x}Sr_xCuO_4}$, maintaining a minimal yet constant surface sensitivity. Contrary to previous results, a significant amount of O $2p_z$ character, ~15% of the O $2p_{x,y}$ character and likely ascribed to apical O, has been observed for both intrinsic and doped holes. The Cu $3d_{3z^2-r^2}$ character is found to be very weak, ~1.5% of the Cu $3d_{x^2-y^2}$ character. The quantitative results impose strong constraints for superconductivity models invoking out-of-plane orbitals, and suggest that the apical O $2p_z$ orbital may play an important role in high-$T_c$ phenomena.

High-quality $\mathrm{La_{2-x}Sr_xCuO_4}$ samples with $x=0.04$, 0.07, 0.15, and 0.34 were grown using off-axis sputter deposition on vicinal $\mathrm{SrTiO_3}$ (101) substrates [10]. Single-domain (103) $\mathrm{La_{2-x}Sr_xCuO_4}$ thin films, ~3500 Å thick with unidirectionally tilted $\mathrm{CuO_2}$ planes, were obtained. The tilt angle between the $c$ axis and the surface normal, $\theta_c$, is 46.3° for $x=0.07$ and 0.15 samples, and is 47.5° for $x=0.04$ and 0.34 samples. X-ray diffraction measured 5000:1, 700:1, 1400:1, and 50:1 for the population ratio of the (103) domain and (103′) antidomains in $x=0.04$, 0.07, 0.15, and 0.34 samples, respectively. The Sr content was determined by both Rutherford backscattering spectroscopy measurements and comparison with the photoabsorption data of ceramic $\mathrm{La_{2-x}Sr_xCuO_4}$ samples [11]. Both methods gave a consistent $x$ within $\pm 0.005$. Transport measurements showed a $T_c(R=0)$ of 5 and 30 K for $x=0.07$ and 0.15 samples, respectively.

The photoabsorption measurements were performed using the AT&T Bell Laboratories Dragon beam line at the National Synchrotron Light Source [12]. The monochromator resolution was set at ~0.15 and ~0.45 eV for the O $K$ edge and Cu $L$ edge, respectively. Bulk-sensitive (~2000 Å probing depth) fluorescence yield (FY) spectra were recorded using a high-sensitivity seven-element germanium array detector. To achieve complete polarization geometry and eliminate optical path variations, an azimuthal rotation method was used; its schematic is shown in Fig. 1. For $\mathbf{E}_h \parallel \mathbf{c}$, the $b$, $c$, and $a$ axes of the $\mathrm{La_{2-x}Sr_xCuO_4}$ thin film are oriented parallel to the incident photon direction, majority polarization vector ($\mathbf{E}_h$), and the minority polarization vector ($\mathbf{E}_v$), respectively. Complete $\mathbf{E}_h \perp \mathbf{c}$ geometry is achieved by rotating the sample about its surface normal, $\mathbf{n}$, by ~150° (exact value depending on $\theta_c$). The fluorescence detector is fixed along the $c$ axis, shown in the figure before rotation, with a collection cone of ±25°. In this arrangement, the optical paths are fixed at nongrazing angles, thus maintaining a minimal yet constant surface sensitivity. Polarization-dependent absorption spectra were then recorded at room temperature as a function of the azimuthal angle $\phi$. After normalization to the incident photon flux, the spectra of different $\phi$ show nearly identical fluores-

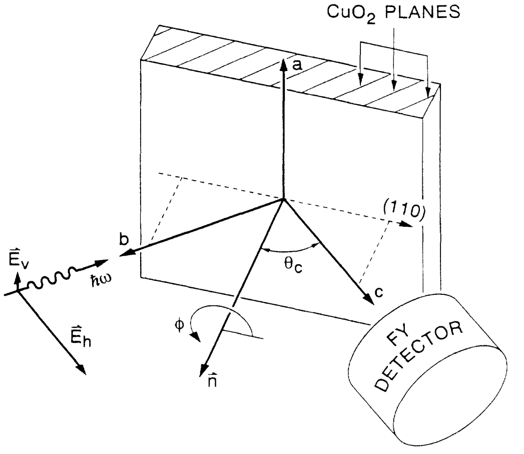

FIG. 1. Geometric arrangement for the $\mathbf{E}_h \parallel \mathbf{c}$ absorption measurements on single-domain (103) $La_{2-x}Sr_xCuO_4$. The $\mathbf{E}_h \perp \mathbf{c}$ geometry can be achieved by rotating the sample about its surface normal, **n**.

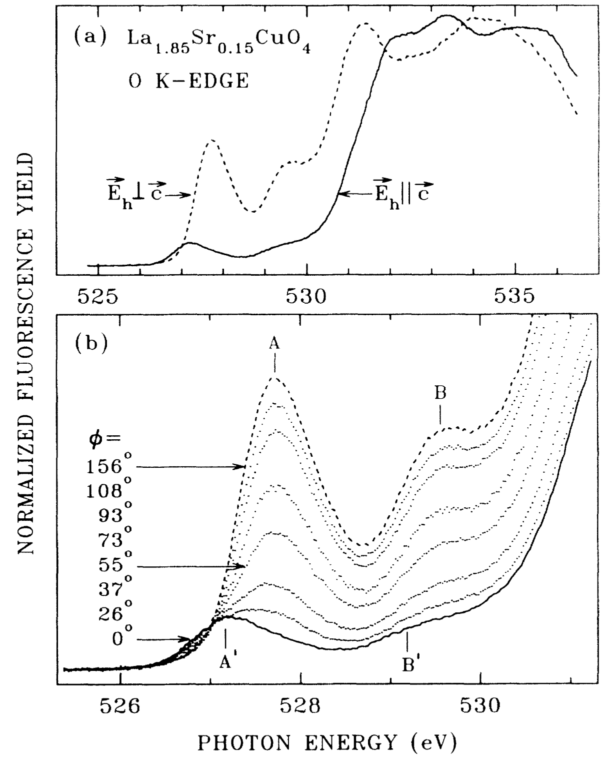

FIG. 2. O $K$-edge fluorescence yield photoabsorption spectra of $La_{1.85}Sr_{0.15}CuO_4$. (a) Wide range spectra for $\mathbf{E}_h \perp \mathbf{c}$ ($\phi = 156°$) and $\mathbf{E}_h \parallel \mathbf{c}$ ($\phi = 0°$); (b) expanded spectra in the low-energy region of (a) and of those taken with intermediate angles. These $\phi$ were chosen such that the value of $|\mathbf{E}_h \times \mathbf{c}|^2/|\mathbf{E}_h|^2$ corresponds to 1.0, 0.9, 0.8, 0.6, 0.4, 0.2, 0.1, and 0.0, respectively.

cence yields at 10 eV below and 100 eV above the edge, where no significant polarization effect is expected. A high degree of linear polarization, $(|\mathbf{E}_h|^2 - |\mathbf{E}_v|^2)/(|\mathbf{E}_h|^2 + |\mathbf{E}_v|^2)$, is obtained by closing the vertical angular acceptance of the synchrotron radiation down to 0.2 mrad. Its upper limit is calculated to be 99%. An independent measurement using a crystal polarimeter at 650-eV photon energy gives a linear polarization of $(98.3 \pm 0.4)\%$.

Figure 2(a) shows the O $K$-edge normalized fluorescence yield absorption spectra for the $x = 0.15$ sample taken with $\mathbf{E}_h \perp \mathbf{c}$ and $\mathbf{E}_h \parallel \mathbf{c}$. Expanded spectra for the low-energy region (peaks labeled $A$ and $B$) as a function of $\phi$ are displayed in Fig. 2(b), showing systematic evolution of the peak intensities. As discussed previously [11], peak $A$ stems from doping-induced holes, and results mainly from a $3d^9\underline{L} \rightarrow \underline{1s}3d^9$ transition; peak $B$ is associated with the "upper Hubbard band" and results from a $3d^9 \rightarrow \underline{1s}3d^{10}$ transition of the undoped material, which is allowed due to the admixture of $3d^{10}\underline{L}$ with $3d^9$ in the ground state. Here $\underline{L}$ and $\underline{1s}$ denote the O $2p_{x,y}$ ligand hole and O $1s$ core hole, respectively. As $\phi$ is changed from $\mathbf{E}_h \perp \mathbf{c}$ to $\mathbf{E}_h \parallel \mathbf{c}$, the intensities of peaks $A$ and $B$ decrease and new peaks (labeled as $A'$ and $B'$) appear at ~0.4 eV lower photon energies, developing full strength at $\mathbf{E}_h \parallel \mathbf{c}$. A dipole transition analysis shows that peak $A$ ($A'$) contains exclusively $2p_{x,y}$ ($2p_z$) character, and gives very good agreement with the observed intensity evolution as a function of $\phi$. The net intensity gain between the $\mathbf{E}_h \parallel \mathbf{c}$ and $\mathbf{E}_h \perp \mathbf{c}$ spectra near 526.8-eV photon energy excludes the possibility of peak $A'$ being an absorption feature due to surface contaminations. The appearance of peak $A'$ clearly demonstrates that the doped holes in $La_{2-x}Sr_xCuO_4$ contain a significant amount of O $2p_z$ character.

Figure 3(a) shows the copper $L_{2,3}$ absorption spectra for the $x = 0.15$ sample taken at $\mathbf{E}_h \perp \mathbf{c}$ and $\mathbf{E}_h \parallel \mathbf{c}$. The $L_3$ spectral region as a function of $\phi$ has been magnified in Fig. 3(b). No energy shift greater than 30 meV is observed at the $L_3$ white line as its intensity reduces by nearly 2 orders of magnitude in going from $\mathbf{E}_h \perp \mathbf{c}$ to $\mathbf{E}_h \parallel \mathbf{c}$ geometry. The raw data of the $L_3$ white line give a $3d_{3z^2-r^2}$ to $3d_{x^2-y^2}$ intensity ratio of 4.5%. After being corrected for the FY saturation effect, this ratio is reduced down to 3% [13]. Figure 3(c) shows the difference spectra obtained by subtracting a small percentage of the intensities of the $\mathbf{E}_h \perp \mathbf{c}$ spectra from those of the $\mathbf{E}_h \parallel \mathbf{c}$ spectra in the $L_2$ white line region. The raw data clearly show that ~3% of the $\mathbf{E}_h \perp \mathbf{c}$ spectrum is sufficient to remove the barely visible $L_2$ white line shown in the $\mathbf{E}_h \parallel \mathbf{c}$ spectra, in excellent agreement with that obtained from the $L_3$ white line with the FY saturation correction. After correction for nonperfect linear polarization $[|\mathbf{E}_v|^2/|\mathbf{E}_h|^2 = (0.9 \pm 0.2)\%]$, analysis of both the $L_3$ and $L_2$ white lines then results in a final value of $(2 \pm 0.5)\%$ for the $3d_{3z^2-r^2}$ to $3d_{x^2-y^2}$ intensity ratio, which is much smaller than previously reported in studies employing different experimental techniques [2,3].

To illustrate the evolution of the O $2p_{x,y}$ and $2p_z$ characters as functions of Sr concentration, Fig. 4(a) shows the low-energy region of the O $K$-edge $\mathbf{E}_h \perp \mathbf{c}$ and $\mathbf{E}_h \parallel \mathbf{c}$ spectra. In the $\mathbf{E}_h \perp \mathbf{c}$ spectra, with increasing Sr doping, peak $A$ gains intensity by introducing holes into the

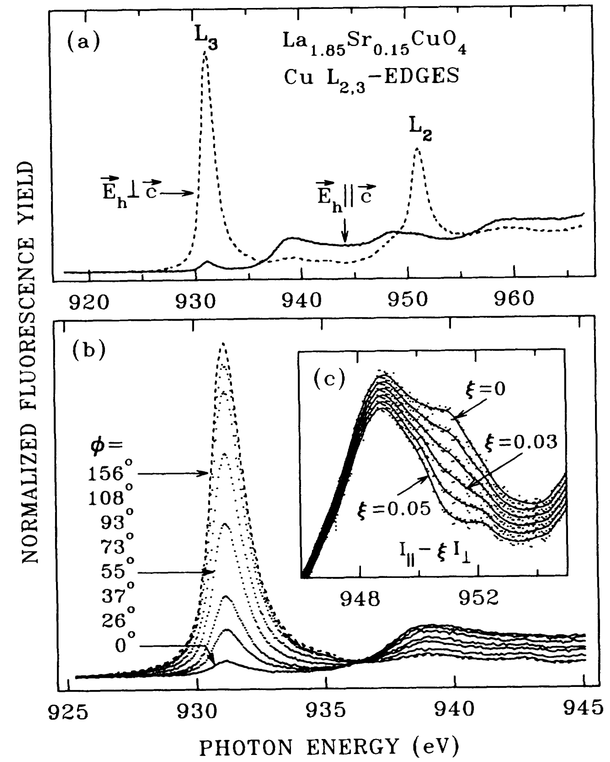

FIG. 3. Cu $L$-edge fluorescence yield photoabsorption spectra of $La_{1.85}Sr_{0.15}CuO_4$. (a) Wide range spectra for $\mathbf{E}_h \perp \mathbf{c}$ ($\phi = 156°$) and $\mathbf{E}_h \parallel \mathbf{c}$ ($\phi = 0°$); (b) expanded spectra in the $L_3$ region of (a) and of those taken with intermediate angles; (c) difference spectra near the $L_2$ white line, obtained by subtracting a small amount ($\xi$) of the intensity of the $\mathbf{E}_h \perp \mathbf{c}$ spectrum from that of the $\mathbf{E}_h \parallel \mathbf{c}$ spectrum.

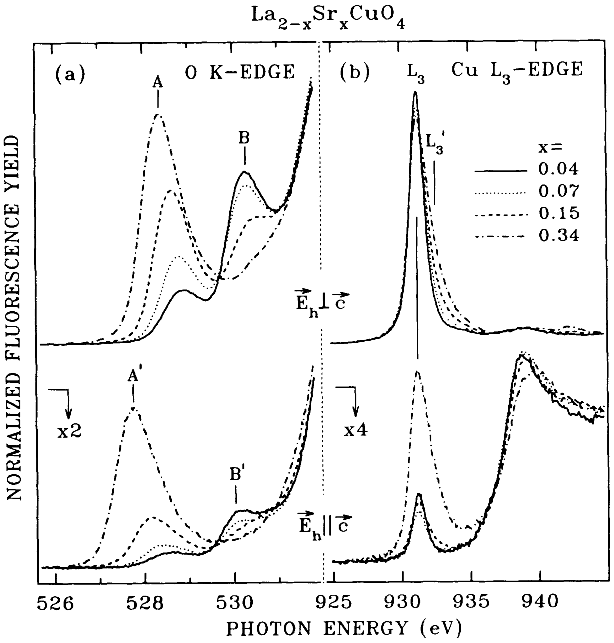

FIG. 4. Fluorescence yield photoabsorption spectra for $\mathbf{E}_h \perp \mathbf{c}$ and $\mathbf{E}_h \parallel \mathbf{c}$ as a function of Sr content. (a) Low-energy region of the O $K$-edge absorption; (b) the $L_3$ white line region of the Cu $L$-edge absorption.

valence states as well as transferring spectral weight from peak $B$ [11]. A similar effect is also observed between peaks $A'$ and $B'$ in the $\mathbf{E}_h \parallel \mathbf{c}$ spectra. The $2p_z$ to $2p_{x,y}$ ratio (peaks $A'$,$A$) is large and varies as $(14 \pm 1)\%$, $(13 \pm 1)\%$, $(16 \pm 1)\%$, and $(34 \pm 2)\%$ for $x = 0.04$, 0.07, 0.15, and 0.34 samples, respectively. Interestingly, this ratio is largest in the sample with highest Sr content. The $2p_z$ to $2p_{x,y}$ intensity ratios for the "upper Hubbard band" (peaks $B'$,$B$) are found to be $(16 \pm 2)\%$ for $x = 0.04$, 0.07, and 0.15 samples; an extrapolation suggests a similar ratio also for the undoped sample ($x = 0$). According to band-structure calculations [14], one may ascribe the $2p_z$ character to apical O, and the $2p_{x,y}$ to in-plane O. The analogous spectral weight transfer from $B'$ to $A'$ ($2p_z$ character), and that from $B$ to $A$ ($2p_{x,y}$ character), strongly suggests that the apical O $2p_z$ mixes with the in-plane O $2p_{x,y}$ and Cu $3d_{x^2-y^2}$ in the ground state, instead of forming a separate band. The 0.3-0.5-eV energy shifts between $2p_z$ and $2p_{x,y}$ character might be due to the differences in the chemical shifts and screening between the apical and in-plane O $1s$ photoabsorption processes.

To investigate the Cu $3d_{3z^2-r^2}$ character, Fig. 4(b) shows the Cu $L_3$ $\mathbf{E}_h \perp \mathbf{c}$ and $\mathbf{E}_h \parallel \mathbf{c}$ spectra for these four samples. Upon Sr doping, the $L_3$ white line in the $\mathbf{E}_h \perp \mathbf{c}$ spectra reduces slightly its peak height and a doping-induced satellite peak (the shoulder indicated as $L_3'$) develops at ~1 eV above the white line. The major configuration involved in the x-ray absorption for the white line and the satellite peak are $3d^9 \rightarrow \underline{2p}_{3/2}3d^{10}$ and $3d^9\underline{L} \rightarrow \underline{2p}_{3/2}3d^{10}\underline{L}$, respectively. Using the aforementioned analysis procedure for the $L_3$ and $L_2$ white lines, the $3d_{3z^2-r^2}$ to $3d_{x^2-y^2}$ intensity ratios for the white line are found to be $(2 \pm 0.5)\%$ for $x = 0.04$, 0.07, and 0.15 samples. For the $x = 0.34$ sample, the ratio increases to $(7.5 \pm 1)\%$, taking into account the presence of ~2% (103) antidomains. By normalizing and subtracting the $L_3$ spectra of the $x = 0.04$ sample from those of the other three samples, the $3d_{3z^2-r^2}$ to $3d_{x^2-y^2}$ intensity ratios of the doping-induced satellite peak ($L_3'$) were estimated to be $(2.5 \pm 1)\%$ for $x = 0.07$ and 0.15 and $(8.5 \pm 2)\%$ for the $x = 0.34$ samples. Considering the larger experimental uncertainties, these ratios are essentially the same as those obtained from the $L_3$ white line, and an extrapolation suggests a similar ratio for the $x = 0.04$ sample as well. Figure 5 summarizes the apical O $2p_z$ to in-plane O $2p_{x,y}$ and the Cu $3d_{3z^2-r^2}$ to $3d_{x^2-y^2}$ intensity ratios of doping-induced peaks.

A careful analysis is required to relate the x-ray absorption intensities to the hole orbital character (occupation numbers) in the ground state. For Cu $3d_{3z^2-r^2}$ to $3d_{x^2-y^2}$ character ratio, the "3/4" factor between $p_{3/2,1/2} \rightarrow d_{x^2-y^2}$ and $p_{3/2,1/2} \rightarrow d_{3z^2-r^2}$ full dipole transition strength needs to be taken into account. After this renormalization, both the intrinsic and doped holes show an apical O $2p_z$ to in-plane O $2p_{x,y}$ character ratio of

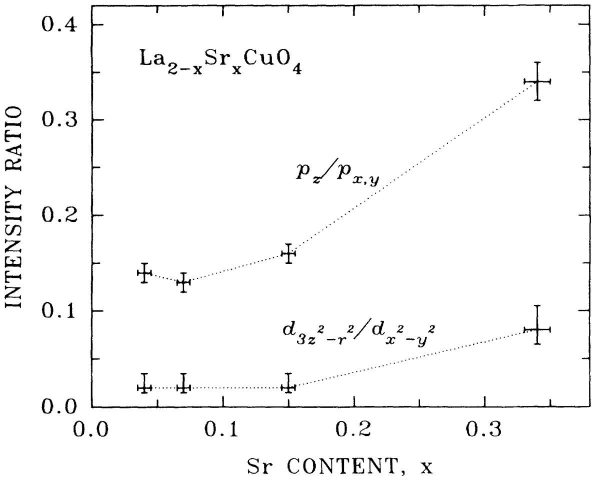

FIG. 5. Apical O $2p_z$ to in-plane O $2p_{x,y}$ and Cu $3d_{3z^2-r^2}$ to $3d_{x^2-y^2}$ intensity ratios of doping-induced peaks as a function of Sr content. The dotted lines serve only as a guide for the eye.

~15% and a Cu $3d_{3z^2-r^2}$ to $3d_{x^2-y^2}$ character ratio of ~1.5% in superconducting samples. Coupling these ratios with the calculated admixture of Cu $3d_{x^2-y^2}$ and in-plane O $2p_{x,y}$ character, one can estimate the Cu $3d_{3z^2-r^2}$ to apical O $2p_z$ character ratio. For intrinsic holes, the calculated admixture is roughly 70% Cu $3d_{x^2-y^2}$ and 30% in-plane O $2p_{x,y}$ [11,14], giving a ~1% Cu $3d_{3z^2-r^2}$ and a ~4% apical O $2p_z$ character. The analysis for the doped holes is more complicated, because it involves a large spectral weight transfer and requires detailed information on the hybridization of various configurations. Nevertheless, knowing that the doped holes contain more in-plane O $2p_{x,y}$ than Cu $3d_{x^2-y^2}$ character (roughly a 3:1 ratio) [11,14], our results indicate that the apical O $2p_z$ is the overwhelmingly predominant out-of-plane orbital for doping-induced holes.

Although the role of the apical O $2p_z$ orbital in high-$T_c$ phenomena is not clear at this time, its prominent appearance and progressive increase relative to the in-plane O $2p_{x,y}$ character with Sr doping could have profound physical implications. For instance, the increase in apical O $2p_z$ to in-plane O $2p_{x,y}$ ratio can enhance the coupling between layers, thus providing an appealing explanation for the rapid increase in out-of-plane to in-plane conductivity ratio with doping [15]. The apical O $2p_z$ orbital may also link directly to the pressure-dependent transport properties [5-8]. Although our data indicate that too large a $2p_z$ to $2p_{x,y}$ ratio may suppress the superconductivity, the arguments on out-of-plane orbitals having a negative influence on superconductivity [9] must confront the significant amount of apical O $2p_z$ character observed in the superconducting samples. The observed very weak Cu $3d_{3z^2-r^2}$ character, on the other hand, imposes a strong constraint on theories requiring a considerable amount of Cu $3d_{3z^2-r^2}$ character, such as in $d$-$d^*$ excitation [7] and triplet hole [8] models.

It is a pleasure to acknowledge useful discussions with B. Batlogg, M. S. Hybertsen, M. Schluter, and J. Zaanen, the technical assistance of G. Meigs and H. J. Lin, and the measurements of the degree of linear polarization by E. Gluskin. Work done at the National Synchrotron Light Source was supported by the DOE under Contract No. DE-AC02-76CH00016.

---

[1] For a bibliography, see F. Al Shamma and J. C. Fuggle, Physica (Amsterdam) **169C**, 325 (1990).

[2] A. Bianconi *et al.*, Solid State Commun. **63**, 1009 (1987); Phys. Rev. B **39**, 3380 (1989); **44**, 10126 (1991); M. Abbate *et al.*, Phys. Rev. B **42**, 7914 (1990); S. Suzuki *et al.*, Phys. Rev. B **44**, 5381 (1991).

[3] N. Nücker *et al.*, Phys. Rev. B **39**, 6619 (1989); H. Romberg *et al.*, Phys. Rev. B **41**, 2609 (1990).

[4] F. J. Himpsel *et al.*, Phys. Rev. B **38**, 11946 (1988); P. Kuiper *et al.*, Physica (Amsterdam) **157B+C**, 260 (1989); H. Matsuyama *et al.*, Physica (Amsterdam) **160C**, 567 (1989); Y. Hirai *et al.*, Phys. Rev. B **45**, 2573 (1992).

[5] T. Egami *et al.*, in *Electron Structure and Mechanisms of High Temperature Superconductivity*, edited by J. Ashkenazi and G. Vezzoli (Plenum, New York, 1991); in Proceedings of Lattice Effects in High $T_c$ Superconductivity, edited by Y. Bar-Yam (World Scientific, Singapore, to be published).

[6] J. G. Bednorz and K. A. Müller, Z. Phys. **64**, 189 (1986); J. Ashkenazi, in *Electron Structure and Mechanisms of High Temperature Superconductivity*, edited by J. Ashkenazi and G. Vezzoli (Plenum, New York, 1991).

[7] W. Weber, Z. Phys. B **70**, 323 (1988); D. L. Cox *et al.*, Phys. Rev. Lett. **62**, 218 (1989).

[8] H. Kamimura and M. Eto, J. Phys. Soc. Jpn. **59**, 3053 (1990); V. I. Anisimov *et al.*, Phys. Rev. Lett. **68**, 345 (1992); J. Zaanen and A. M. Oles (to be published).

[9] Y. Ohta, T. Tohyama, and S. Maekawa, Phys. Rev. B **43**, 2968 (1991); C. Di Castro, L. F. Feiner, and M. Grilli, Phys. Rev. Lett. **66**, 3209 (1991).

[10] J. Kwo, R.M. Fleming, H. L. Kao, D. J. Werder, and C.H. Chen, Appl. Phys. Lett. (to be published).

[11] C. T. Chen *et al.*, Phys. Rev. Lett. **66**, 104 (1991); H. Eskes, M. B. J. Meinders, and G. A. Sawatzky, Phys. Rev. Lett. **67**, 1035 (1991).

[12] C. T. Chen, Nucl. Instrum. Methods Phys. Res., Sect. A **256**, 595 (1987); C. T. Chen and F. Sette, Rev. Sci. Instrum. **60**, 1616 (1989).

[13] For the $L_3$ white line in $\mathbf{E}_h \perp \mathbf{c}$ spectra, a $I_m I(\lambda)/[I_m - I(\lambda)]$ functional form correction for the FY saturation effect is needed. Three different methods were utilized and a consistent $I_m$ of ~3 times the peak height of the $L_3$ white line was obtained. For the low-energy peaks at the O $K$ edge and for the Cu $L_2$ white line, this correction is not essential because their absorption cross sections are quite small compared to the total absorption cross sections of the samples.

[14] M. S. Hybertsen, M. Schluter, and N. E. Cristensen, Phys. Rev. B **39**, 9028 (1989); A. K. McMahan, J. F. Annett, and R. M. Martin, Phys. Rev. B **42**, 6268 (1990); J. B. Grant and A. K. McMahan, Phys. Rev. Lett. **66**, 488 (1991).

[15] S. Kambe *et al.*, Physica (Amsterdam) **160C**, 35 (1989).